

Spatiotemporal Self-Organization of Fluctuating Bacterial Colonies

Tobias Grafke,¹ Michael E. Cates,² and Eric Vanden-Eijnden¹

¹*Courant Institute, New York University, 251 Mercer Street, New York, NY 10012, USA*

²*DAMTP, Centre for Mathematical Sciences, Wilberforce Road, Cambridge, CB3 0WA, United Kingdom*

(Dated: May 6, 2022)

We model an enclosed system of bacteria, whose motility-induced phase separation is coupled to slow population dynamics. Without noise, the system shows both static phase separation and a limit cycle, in which a rising global population causes a dense bacterial colony to form, which then declines by local cell death, before dispersing to re-initiate the cycle. Adding fluctuations, we find that static colonies are now metastable, moving between spatial locations via rare and strongly nonequilibrium pathways, whereas the limit cycle becomes quasi-periodic such that after each redispersion event the next colony forms in a random location. These results, which resemble some aspects of the biofilm-planktonic life cycle, can be explained by combining tools from large deviation theory with a bifurcation analysis in which the global population density plays the role of control parameter.

PACS numbers: 87.10.Mn, 87.17.Jj, 05.40.-a

Because they are not bound by the standard laws of equilibrium thermodynamics, active materials such as bird flocks [1], motile bacteria [2], self-organizing bio-polymers [3, 4], or man-made self-propelled particles [5] have many more routes towards self-assembly and self-organization than systems whose dynamics satisfy detailed-balance. While much remains to be done to build a statistical mechanics theory of these non-equilibrium systems, some generic principles governing their behavior have started to emerge. Motility-induced phase separation (MIPS) is one example [6, 7]. MIPS arises naturally in systems of self-propelled particles whose locomotive speed decreases strongly at high density, through a feedback in which particles accumulate where they move slowly and vice-versa. This provides a generic route to pattern formation in motile agents, including both micro-organisms such as *E. coli* [8, 9], where slowdown can be caused by quorum sensing [10–13], and synthetic colloidal analogues where slowdown is caused by crowding [7, 14–17]. The simplest theories of MIPS effectively describe thermodynamic phase separation, and are governed by an effective free energy functional [7], although this does not hold in general as active gradient terms can alter the coexistence behavior [6, 7].

MIPS, or for that matter thermodynamic phase separation caused by attractions, can be arrested by the birth and death of particles. The simplest (logistic) population dynamics has for uniform systems a stable fixed point at some carrying capacity ρ_0 , with decay towards this from higher or lower densities. If ρ_0 lies within the miscibility gap of a phase separation, the uniform state at ρ_0 is unstable, but so is a state of coexisting bulk phases (each of which would have nonstationary density). This can result in stationary patterns of finite wavelength, in which bacteria reproduce in dilute regions, migrate by diffusive motility to dense ones, become immotile, and there die off by overcrowding [7, 18]. In [18] a field theoretic description of such arrested phase separation was proposed. This is perhaps the simplest physical model to capture the variety of bacterial colony patterns earlier observed in experiments [19].

However, the work of [18] describes only stationary spatial

rather than spatiotemporal patterns, and it crucially neglects the effects of intrinsic fluctuations in population density and motility of the bacteria. These fluctuations are always present in finite systems and they are relevant to the nature and stability of the self-assembling structures. The purpose of the present Letter is to quantify these effects in situations where birth and death processes are slow compared to diffusive exploration times. For simplicity we focus on one-dimensional systems whose extent is smaller than the natural length scale for the spacing between dense patches, set by the distance a particle can move during its lifetime. Accordingly, only one dense bacterial domain of low motility (hereafter ‘colony’) is present at a time, with the remaining bacteria in a dilute and motile (i.e., ‘planktonic’) phase. This simplification allows us to focus on temporal aspects of the pattern formation, and also to give a thorough analysis of the role of noise terms. Our qualitative conclusions, however, should apply in higher dimensions; larger domains will be discussed elsewhere [20].

Concretely, we identify two regimes in which the fluctuations induce nontrivial self-organization pathways. The first arises in situations where the deterministic dynamics possess time-periodic solutions driven by the interplay between MIPS and the competition for resources: in the resulting limit cycles a colony of bacteria periodically appears and disappears at a fixed location in the domain. In this regime, the fluctuations, no matter how small, are shown to have a drastic impact on this process: they allow the colony to explore its environment by randomly jumping from one location to another each time the system revisits its spatially homogeneous planktonic state. With periodic spatial boundary conditions the colony now appears and disappears at spatially random locations; if boundary conditions instead favor localization at container walls, a random choice of wall is made each cycle. It is striking that this behavior, which resembles the biofilm-planktonic lifecycle of several micro-organisms [21] can arise from the combination of MIPS and logistic growth alone – particularly as the bacterial quorum sensing response, a likely cause of MIPS [9, 18] is now thought also to be directly implicated in biofilm disper-

sion [13]. We are not suggesting that the combination of MIPS and logistic growth directly explains the complex life cycle of real biofilms, but it may nonetheless be a contributory factor in its evolution from simpler beginnings.

In our second regime, the deterministic theory predicts a single static colony with multiple stable locations. In these situations the intrinsic fluctuations induce rare, noise-activated transitions via the uniform state from one such metastable pattern to another. (This again resembles the biofilm lifecycle referred to above, but now with random intervals between dispersion events.) As shown below, the rate and mechanism of these transitions can be completely characterized using tools from large deviation theory [22]. The transition pathways are intrinsically out-of-equilibrium and involve a subtle interplay between phase-separation and reproduction. In particular these transitions do not follow the deterministic relaxation path in reverse, as one would predict from standard equilibrium arguments in systems with microscopic reversibility.

Following [18], we focus on motile bacteria whose motile diffusivity $D(\rho) = v^2(\rho)\tau/d$ [9] depends on their local density ρ via the swim speed $v(\rho)$. Here τ is a rotational relaxation time and d is dimensionality. Because the swim speed varies in space through ρ , the particles have a mean drift velocity $\mathbf{V}(\rho) = -\frac{1}{2}D'(\rho)\nabla\rho$ [9]. Neglecting fluctuations, these effects can be combined into the following equation governing the evolution of the bacterial density $\rho(\mathbf{x}, t)$:

$$\partial_t \rho = \nabla \cdot (\mathcal{D}_e(\rho)\nabla\rho) - \delta^2 \nabla \cdot (\rho D(\rho)\nabla\Delta\rho). \quad (1)$$

In this equation the diffusivity and drift have been combined into a collective diffusivity $\mathcal{D}_e(\rho) = D(\rho) + \frac{1}{2}\rho D'(\rho)$, and a higher-order gradient, or regularizing, term proportional to δ^2 has been added to account for the fact that the bacteria only sense each other's influence over a finite distance $\delta > 0$ [23].

Our choice of regularizer, which differs from that of [18], allows (1) to be cast as an effective equilibrium model. That is, when a fluctuating noise term is added to (1), the resulting equation is in detailed balance (DB) with the free energy

$$F[\rho] = \int_{\Omega} (\rho \log \rho - \rho + f(\rho) + \frac{1}{2}\delta^2 |\nabla\rho|^2) d\mathbf{x}, \quad (2)$$

where $f'(\rho) = \log D(\rho)/2$, even though the underlying microscopic dynamics are not. Eq. (1) then takes the form of a generalized gradient flow, $\partial_t \rho = -M(\rho)(\delta F/\delta\rho)$, with nonlinear mobility operator $M(\rho)\xi = \nabla \cdot (\rho D(\rho)\nabla\xi)$ [24]. The DB property is destroyed by the birth and death terms addressed below, but simplifies the analysis when these are small.

Crucially, whenever $d \ln v/d \ln \rho < -1$, we have $\mathcal{D}_e(\rho) < 0$ in (1). This is the spinodal regime of local instability for MIPS [9]. To explore this in a finite spatial domain, it is useful to make the model specific. Following [18] we assume an exponential form, $v(\rho) = v_0 e^{-\lambda\rho/2}$ where v_0 is the speed of an isolated particle and $\lambda > 0$. This gives $\mathcal{D}_e(\rho) = \tau v_0^2 e^{-\lambda\rho}(1 - \frac{1}{2}\lambda\rho)$. In a d -dimensional box $\Omega = [0, L]^d$, after non-dimensionalization via $\tau v_0^2 = \lambda = 1$, (1) reduces to

$$\partial_t \rho = \nabla \cdot \left((1 - \frac{1}{2}\rho)e^{-\rho}\nabla\rho - \delta^2 \rho e^{-\rho}\Delta\nabla\rho \right). \quad (3)$$

We study (3) for $\mathbf{x} \in \Omega = [0, 1]^d$ with, unless otherwise stated, Neumann boundary conditions: $\hat{\mathbf{n}} \cdot \nabla\rho = 0 \forall \mathbf{x} \in \partial\Omega$ for $\hat{\mathbf{n}}$ normal to the boundary. These localize the dense phase at a wall, to minimize its interfacial energy.

The mean bacterial density, $\bar{\rho} = |\Omega|^{-1} \int_{\Omega} \rho(\mathbf{x}) d\mathbf{x}$, is conserved by (3) and controls the phase separation. Fig. 1 (left) shows the bifurcation diagram obtained when $d = 1$ and $\delta^2 = 2 \cdot 10^{-3}$ by projecting the fixed points of (3) onto the $(\bar{\rho}, A)$ plane, where the ‘signed asymmetry’ $A[\rho] = \pm(\int_0^1 (\rho(x) - \rho(1-x))^2 dx)^{1/2}$ is taken positive when the high density phase is located on the left side of the box. A linear stability analysis finds the spatially uniform solution to be stable if $\bar{\rho} < \rho_S = 2/(1 - 2\delta^2\pi^2)$. (This becomes the bulk spinodal condition in the large system, or small δ , limit.) A subcritical pitchfork bifurcation occurs at $\bar{\rho} = \rho_S$, where two unstable and one stable branches merge into a single unstable branch. The remaining two stable branches, $\rho_L(x)$ and $\rho_R(x)$ correspond to colony formation on either the left or the right wall. Once present, each such phase-separated state remains stable down to a ‘binodal’ density $\bar{\rho} = \rho_B < \rho_S$ [25], whereas for $\bar{\rho} < \rho_B$ the colony redisperses diffusively.

These transitions in static stability become *dynamically* significant once the mean bacterial density $\bar{\rho}$ is allowed to change by introducing logistic growth. Focusing again on the deterministic situation first, this adds to (3) a term $\alpha\rho(1 - \rho/\rho_0)$, where α is the birth rate and ρ_0 is the carrying capacity. Crucially, this breaks detailed balance, allowing not only steady-state fluxes [18] but also nonstationary patterns (see below). When the population dynamics is much slower than particle motion, $\alpha \ll 1$, the bifurcation diagram shown in Fig. 1 now depicts the projection of a *slow manifold* \mathcal{M} instead. Diffusive motility leads to convergence of ρ to \mathcal{M} on a fast time-scale, of order 1 in α , during which the global mean $\bar{\rho}$ is almost conserved. On \mathcal{M} itself, the motion is driven solely by changing $\bar{\rho}$ via the slow logistic term on time-scales of order α^{-1} .

Three different regimes can then be identified on varying the carrying capacity ρ_0 . For $\rho_0 < \rho_S$ the system remains in a uniform phase, in which dilute motile bacteria homogeneously cover the domain at $\rho(x) = \rho_0$ [26]. Beyond this point homogeneous solutions cannot exist, and the solution jumps to one of the stable branches, leading to a dense layer of immotile bacteria at one of the boundaries, which forms on the fast, $O(1)$ time-scale. However, for carrying capacities $\rho_S < \rho_0 < \rho_0^c$, the resulting colony is destabilized by the birth/death term; two limit cycles then appear. As soon as a colony emerges at one end of the domain, the bacteria in it start to slowly die out until the global density drops again to ρ_B [27].

It then disperses rapidly, reverting to a uniform phase, whose density then slowly grows until ρ_S is again reached and the cycle begins anew. Symmetry is broken by weak memory of the previous cycle, so that the colony always reforms in the same place. (This also holds with periodic boundary conditions; but the location is then arbitrary.) One of these limit cycles is projected onto the bifurcation diagram in Fig 1 (left), and its spatio-temporal evolution shown in Fig. 1 (right, a).

Finally, for $\rho_0 > \rho_0^c$, all stable fixed points of the system

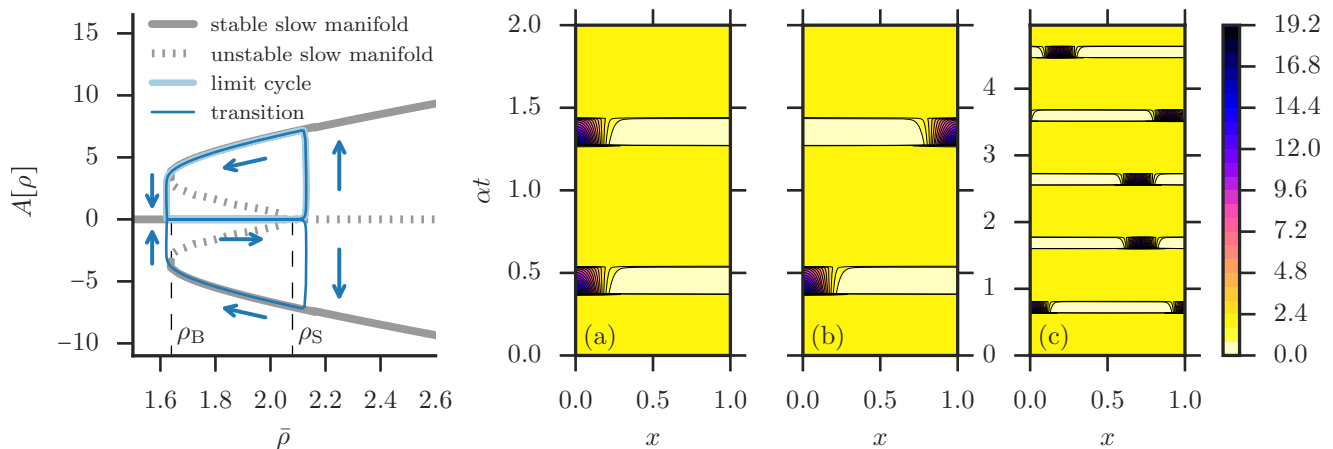


FIG. 1. *Left panel*: Bifurcation diagram in a 2-dimensional projection. The x -axis shows the spatial mean of ρ , the y -axis shows its signed asymmetry $A[\rho]$ (see text for details). For carrying capacities $\rho_B < \rho_0 < \rho_0^c$, no stable fixed point of the dynamics exist. A limit cycle (light blue) and a trajectory with a small amount of noise (dark blue) that exhibits a transition to the lower stable branch are projected into the diagram. *Right panels (a), (b), and (c)*: The time-evolution of the limit cycle with a colony located at the left boundary (upper cycle on the left panel) is shown in subplot (a). Fluctuations allow the solution to randomly jump between the limit cycles with colonies located at the left or right of the domain, as shown in subplot (b). Subplot (c) depicts the quasi-periodic regime in a spatially periodic domain, where the fluctuations randomize the colony location.

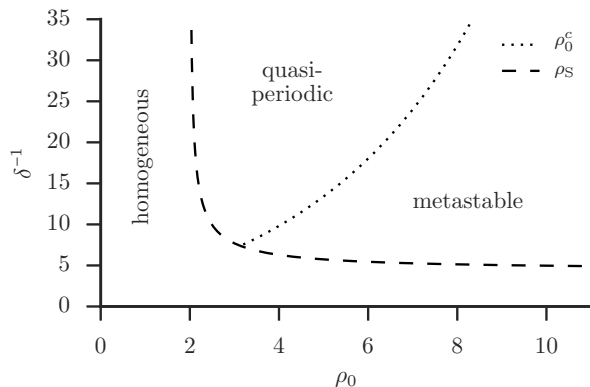


FIG. 2. Phase diagram a function of ρ_0 and δ , showing regimes with homogeneous, quasi-periodic, and metastable solutions. The dashed line shows $\rho_S = 2/(1 - 2\delta^2\pi^2)$, the dotted line ρ_0^c .

comprise a dense colony in coexistence with a planktonic ‘vapor’. A steady flux of particles from the vapor balances cell-death within the colony, so that the macroscopic model is stationary, while the microscopic dynamics are not [18]. Such fixed points correspond to points on stable branches of the slow manifold \mathcal{M} . For $d = 1$ there are two such branches ($\rho_{L,R}$), with more in $d \geq 2$, corresponding to (say) colonies located in the corners of a square in $d = 2$. For these computations and the ones below, we picked $\alpha = 10^{-4}$ and $\delta^2 = 2 \cdot 10^{-3}$, which leads to $\rho_S \approx 2.08$, $\rho_B \approx 1.64$, and $\rho_0^c \approx 6.749$. The complete phase diagram in δ and ρ_0 is shown in Fig. 2.

So far we have neglected the effect of intrinsic fluctuations, both in the diffusive and the reproductive dynamics, which

are always present because the number of bacteria is finite. The fluctuations in diffusion can be formally accounted for by adding in (3) a noise-term $\sqrt{\epsilon}\nabla \cdot (\sqrt{\rho}D(\rho)\boldsymbol{\eta})$, where $\boldsymbol{\eta}$ is spatio-temporal white noise and $\epsilon \propto \bar{\rho}/N$ is a small parameter connecting the (dimensionless) global density to the actual number of particles N present in the domain Ω . On the other hand, the population dynamics can be modeled by a reversible reaction $A \leftrightarrow A + A$ with forward and backward rates $r_f \sim \alpha$ and $r_b \sim \alpha/\rho_0$ [28]. The combined effect is captured by a Markov jump process. In the limit $\epsilon \rightarrow 0$, this gives the logistic growth term $\alpha\rho(1 - \rho/\rho_0)$ considered before, with fluctuations that are Poisson at each location, scaling again with $\sqrt{\epsilon}$ [29].

We consider only the weak fluctuation regime ($\epsilon \ll 1$, or large N) which can be captured by large deviation theory (LDT) [22]. This theory predicts that a noise-driven event occurs, with probability close to 1, via the path involving the least unlikely fluctuation able to drive this event. The resulting most likely path (MLP, also referred to as the *instanton*) is the minimizer of the action functional

$$S_T[\rho] = \frac{1}{2} \int_0^T dt \int_{\Omega} d\mathbf{x} \theta(\mathbf{x}, t; \rho) \partial_t \rho(\mathbf{x}, t) \quad (4)$$

which quantifies the likelihood of the ‘fluctuation’ $\theta(\mathbf{x}, t; \rho)$. In our context, $\theta(\mathbf{x}, t; \rho)$ is related to $\rho(\mathbf{x}, t)$ via [30]

$$\begin{aligned} \partial_t \rho = & \nabla \cdot (\mathcal{D}_e(\rho)\nabla\rho - \rho D(\rho)\nabla(\delta^2\Delta\rho + \theta)) \\ & + \alpha\rho(1 - \rho/\rho_0) + \alpha\rho e^\theta - \alpha\rho^2 e^{-\theta}/\rho_0. \end{aligned} \quad (5)$$

The action S_T should be minimized over all paths, and all durations T , consistent with the event of interest, giving $S^* = \inf_{T>0} \inf_{\rho} S_T[\rho]$. The minimizer is the MLP for the event, whose rate is then, up to a prefactor, $\exp(-\epsilon^{-1}S^*)$ [31].

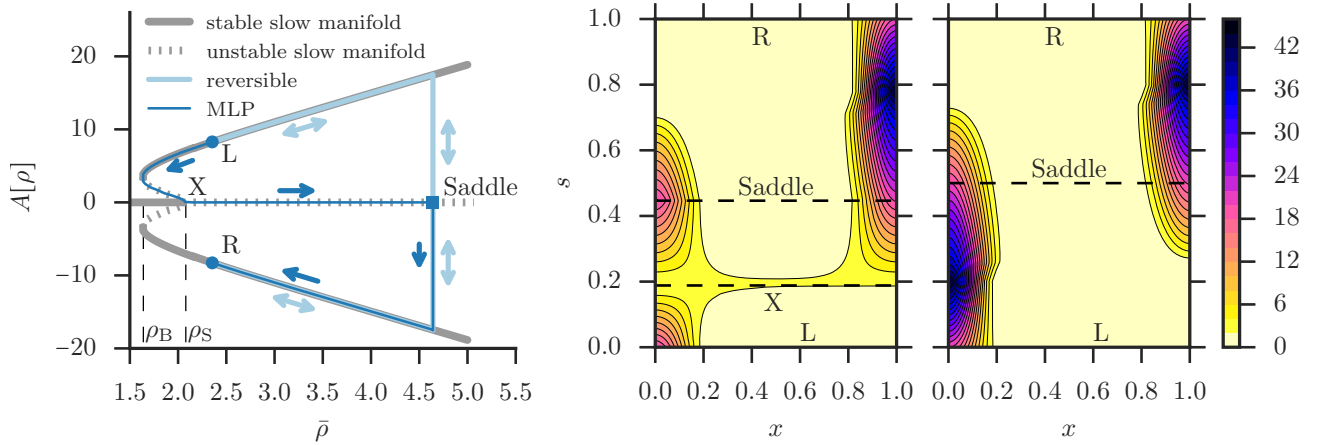


FIG. 3. Transition paths between ρ_L and ρ_R . Here, $x \in [0, 1]$ denotes the spatial extend and $s \in [0, 1]$ the normalized arc-length along each trajectory. *Left*: Projection into bifurcation diagram, see Fig. 1. *Center*: MLP from ρ_L to ρ_R . *Right*: Reversible transition from ρ_L to ρ_R .

In the regime $\rho_0 < \rho_S$, the spatially homogeneous configuration is stable and LDT predicts that deviations away from it are exponentially rare and transient. This is no longer true for $\rho_S < \rho_0 < \rho_0^c$: Since part of the limit cycle tracks $O(\alpha)$ close to the separatrix $\rho(x) = \text{const.}$ for times of order $O(\alpha^{-1})$, even tiny fluctuations can trigger a crossing of the separatrix into the other limit cycle. This is consistent with the LDT picture, which indicates that, in the limit $\alpha \rightarrow 0$, zero-action minimizers exist that connect these two limit cycles. Therefore, due to the fluctuations, bacterial colonies randomly appear either on the left or on the right side of the domain, only to disappear again after times of order $O(\alpha^{-1})$. This switching behavior is depicted in Fig. 1 (b). With periodic boundary conditions, the colony instead appears at a random location each cycle, as shown in Fig. 1 (c). Note that the time period of the cycles is not affected significantly by these fluctuations.

For $\rho_0 > \rho_0^c$, on the other hand, the deterministically stable states ρ_L and ρ_R become metastable; the noise triggers rare and aperiodic transitions between them. A projection of the resulting MLP from ρ_L to ρ_R onto the bifurcation diagram is shown in Fig. 3 (left), whereas its actual shape is shown in Fig. 3 (center); that from ρ_R to ρ_L follows by symmetry. To understand its features, notice that the slow manifold connects the two stable fixed points ρ_L and ρ_R through the bifurcation point, and so can be used as a channel to facilitate the transition. This is indeed correct for $\delta \ll 1$, as the free energy barrier for a jump between stable branches scales like δ^{-1} [20]. It is confirmed by a numerical calculation of the MLP as shown in Fig. 3 (center): The colony of bacteria on the left first disperses to form a uniform planktonic phase which then attains the bifurcation point $\rho_X(x) = \rho_S$. The system then follows the unstable branch (separatrix) of \mathcal{M} – with two symmetric colonies – to the saddle point at $\rho_{\text{Saddle}}(x)$, where it enters the basin of attraction of ρ_R . As seen in its projection onto the bifurcation diagram (Fig. 3) the MLP uses solely the slow manifold: no jump between branches of \mathcal{M} is involved. Note that for finite ϵ , dif-

usive noise will push the actual trajectory off the separatrix well before it reaches the transition state at ρ_{Saddle} . The event rate is still found by LDT, since the motion after visiting ρ_X is effectively deterministic: only the part of the MLP joining ρ_L to ρ_X contributes to the action S^* . In the metastable regime, the transition $\rho_L \leftrightarrow \rho_R$ is exponentially rare.

To emphasize the non-equilibrium nature of this transition, we contrast its MLP with that predicted by a naive equilibrium argument: If the system were in detailed balance, time-reversal symmetry would require the transition path to follow the deterministic relaxation trajectory in reverse from ρ_L to the transition state ρ_{Saddle} , and then relax deterministically to ρ_R . The MLP for reversible systems is thus the heteroclinic orbit connecting the metastable fixed points. Fig. 3 depicts the reversible trajectory for $\rho_L \rightarrow \rho_R$ (right) and its projection (left). Along this trajectory, the colony initially grows instead of shrinking, bringing the global average density $\bar{\rho}$ up to ρ_{Saddle} . Subsequently, bacteria leave the colony, cross the low-density region in the center, and accumulate on the opposite wall, keeping $\bar{\rho}$ constant. This part of the transition happens diffusively causing the system to leave the slow manifold. After passing through ρ_{Saddle} , the reversible transition necessarily coincides with the true MLP. Both are projected into the bifurcation diagram Fig. 3 for comparison.

In summary, we have analyzed a minimal model for the fluctuating dynamics of self-organization among motile bacteria in a finite domain, in the presence of birth and death processes that are slow compared to diffusive time-scales. For $\rho_S < \rho_0 < \rho_0^c$, a bacterial colony is present; fluctuations allow it to explore the domain by random relocation at regular intervals. This exploration remains possible at higher carrying capacities, $\rho_0 > \rho_0^c$, where fluctuations now induce rare, aperiodic relocations. Such transitions are inherently out-of-equilibrium: their most likely path differs significantly from the one followed in systems with time-reversible dynamics.

In our model, relocation of a colony is triggered by a slow

decline in local population density, followed by rapid dispersal into the planktonic state and re-formation elsewhere, rather than by progressive migration between old and new sites. The intermediate state has no colonies in the first case and two in the second – alternatives that should be clearly distinguishable experimentally [32]. Similar considerations may apply to other organisms that alternate between nomadic and cooperative lifestyles. The analytical and numerical tools used here should also be useful in these and other non-equilibrium systems in which noise-driven self-organization occurs.

Acknowledgments. We thank T. Schäfer for his help with the numerical scheme and A. Donev, O. Hirschberg, and C. Nardini for interesting discussions. MEC is funded by the Royal Society. EVE is supported in part by the Materials Research Science and Engineering Center (MRSEC) program of the National Science Foundation (NSF) under award number DMR-1420073 and by NSF under award number DMS-1522767.

-
- [1] M. Ballerini, N. Cabibbo, R. Candelier, A. Cavagna, E. Cisbani, I. Giardina, V. Lecomte, A. Orlandi, G. Parisi, A. Procaccini, M. Viale, and V. Zdravkovic, *Proceedings of the National Academy of Sciences* **105**, 1232 (2008).
- [2] M. C. Marchetti, J. F. Joanny, S. Ramaswamy, T. B. Liverpool, J. Prost, M. Rao, and R. A. Simha, *Reviews of Modern Physics* **85**, 1143 (2013).
- [3] V. Schaller, C. Weber, C. Semmrich, E. Frey, and A. R. Bausch, *Nature* **467**, 73 (2010).
- [4] Y. Sumino, K. H. Nagai, Y. Shitaka, D. Tanaka, K. Yoshikawa, H. Chaté, and K. Oiwa, *Nature* **483**, 448 (2012).
- [5] J. R. Howse, R. A. L. Jones, A. J. Ryan, T. Gough, R. Vafabakhsh, and R. Golestanian, *Physical Review Letters* **99**, 048102 (2007).
- [6] R. Wittkowski, A. Tiribocchi, J. Stenhammar, R. J. Allen, D. Marenduzzo, and M. E. Cates, *Nature Communications* **5**, 4351 (2014).
- [7] M. E. Cates and J. Tailleur, *Annual Review of Condensed Matter Physics* **6**, 219 (2015).
- [8] J. A. Shapiro, *BioEssays* **17**, 597 (1995).
- [9] J. Tailleur and M. E. Cates, *Physical Review Letters* **100**, 218103 (2008).
- [10] M. R. Parsek and E. P. Greenberg, *Trends in Microbiology* **13**, 27 (2005).
- [11] C. Liu, X. Fu, L. Liu, X. Ren, C. K. L. Chau, S. Li, L. Xiang, H. Zeng, G. Chen, L.-H. Tang, P. Lenz, X. Cui, W. Huang, T. Hwa, and J.-D. Huang, *Science* **334**, 238 (2011).
- [12] X. Fu, L.-H. Tang, C. Liu, J.-D. Huang, T. Hwa, and P. Lenz, *Physical Review Letters* **108**, 198102 (2012).
- [13] C. Solano, M. Echeverez, and I. Lasa, *Current Opinion in Microbiology Cell regulation*, **18**, 96 (2014).
- [14] Y. Fily and M. C. Marchetti, *Physical Review Letters* **108**, 235702 (2012).
- [15] J. Palacci, S. Sacanna, A. P. Steinberg, D. J. Pine, and P. M. Chaikin, *Science* **339**, 936 (2013).
- [16] I. Buttinoni, J. Bialké, F. Kümmel, H. Löwen, C. Bechinger, and T. Speck, *Physical Review Letters* **110**, 238301 (2013).
- [17] M. E. Cates and J. Tailleur, *EPL (Europhysics Letters)* **101**, 20010 (2013).
- [18] M. E. Cates, D. Marenduzzo, I. Pagonabarraga, and J. Tailleur, *Proceedings of the National Academy of Sciences* **107**, 11715 (2010).
- [19] J. Murray, *Mathematical Biology II: Spatial Models and Biochemical Applications, volume II* (Springer-Verlag, 2003).
- [20] T. Grafke, O. Hirschberg, and E. Vanden-Eijnden, “Stochastic thermodynamics of reproducing, motile bacteria,” (2017), in preparation.
- [21] M. Kostakioti, M. Hadjifrangiskou, and S. J. Hultgren, *Cold Spring Harbor Perspectives in Medicine* **3**, a010306 (2013).
- [22] M. I. Freidlin and A. D. Wentzell, *Random perturbations of dynamical systems*, Vol. 260 (Springer, 2012).
- [23] In general this effect leads to a nonlocal equation, out of which (1) emerges at leading order after expansion in $\delta > 0$. For details, see [20].
- [24] A. Mielke, D. R. M. Renger, and M. A. Peletier, *Journal of Non-Equilibrium Thermodynamics* **41**, 141 (2016).
- [25] For the particular choice in (3), $\rho_B \rightarrow 0$ in the large system limit but for a finite system the lower stability limit $\rho_B < \rho_S$ remains nonzero, albeit now depending on $\bar{\rho}$ as well as δ .
- [26] Note that for $\rho_B < \rho_0 < \rho_S$, the two phase separated states $\rho_{L,R}$ are destabilized by the α term.
- [27] A *permanent* conversion to an immotile phenotype may have similar effects to cell death for these purposes, since only motile individuals contribute to the dynamical equilibrium between the colony and its planktonic vapor.
- [28] In a system without other interactions, this would not break detailed balance. But detailed balance under (1) would require nonconstant rates such that $\ln(\rho_b/r_f) \propto \delta F/\delta \rho$.
- [29] A. Shwartz and A. Weiss, *Large Deviations For Performance Analysis: Queues, Communication and Computing* (CRC Press, 1995).
- [30] The structure of the noise terms present in the system can be read off (5). Their combined correlation results in a single fluctuation variable $\theta(\mathbf{x}, t; \rho)$, as discussed in [20].
- [31] Note that these calculations necessitate to send $T \rightarrow \infty$, which poses a numerical difficulty that can be avoided by reformulating the problem geometrically and parametrizing the paths by their normalized arc-length rather than physical time. This leads to the geometric minimum action method, which is what we used here: we refer the reader to [33, 34] for details.
- [32] Use of a chemostat for nutrients should allow a spatially uniform carrying capacity ρ_0 to be maintained as required.
- [33] M. Heymann and E. Vanden-Eijnden, *Communications on Pure and Applied Mathematics* **61**, 1052 (2008).
- [34] T. Grafke, T. Schäfer, and E. Vanden-Eijnden, arXiv:1604.03818 [cond-mat] (2016).